Optical Engineering

SPIEDigitalLibrary.org/oe

# Dual-parameter sensor based on a no-core fiber and fiber Bragg grating

Guei-Ru Lin
Ming-Yue Fu
Cheng-Ling Lee
Wen-Fung Liu

# Dual-parameter sensor based on a no-core fiber and fiber Bragg grating

**Guei-Ru Lin,[a,*] Ming-Yue Fu,[b] Cheng-Ling Lee,[c] and Wen-Fung Liu[d]**
[a]Feng-Chia University, Ph.D. Program in Electrical and Communications Engineering, No. 100, Wenhwa Road, Seatwen, Taichung 40724, Taiwan
[b]Air Force Academy, Department of Avionics Engineering, No. Sisou 1, Jieshou W. Road, Gangshan District, Kaohsiung 82047, Taiwan
[c]National United University, Department of Electro-Optical Engineering, No. 1, Lienda Miaoli 36003, Taiwan
[d]Feng-Chia University, Department of Electrical Engineering, No. 100, Wenhwa Road, Seatwen, Taichung 40724, Taiwan

**Abstract.** A dual-parameter fiber sensor achieved by cascading a fiber Bragg grating with a no-core fiber (NCF) is used for simultaneously detecting both the temperature and index physical parameters. The main index sensing mechanism of NCF is based on the wavelength shift of multimode signals' interference (MMI), and the temperature-sensing mechanism is determined by the Bragg wavelength shift and MMI wavelength shift. As the testing index value approaches the cladding index of the optical fiber, an MMI-induced loss-dip is thus created with a sensitivity of 899 nm/RIU due to the phase-match condition of MMI being satisfied. By coating the thin films of different materials, this kind of sensor can be applied in a wide range of different sensing systems.  [DOI: 10.1117/1.OE.53.5.050502]

Keywords: optical fiber sensor; multimode interference; temperature; refractive index measurement; fiber Bragg grating.

Paper 140373L received Mar. 6, 2014; revised manuscript received Apr. 19, 2014; accepted for publication May 2, 2014; published online May 20, 2014.

## 1 Introduction

Optical fiber sensors have become potentially useful for a wide range of sensing applications for their various physical parameter measurements.[1–4] Due to the inherently different optical properties from the fiber Bragg grating (FBG) and long period grating (LPG), the related parameters such as strain, temperature, and refractive index can be measured simultaneously.[5–7] For instance, a hybrid configuration LPG-FBG sensor was fabricated by UV writing in a D fiber for increasing the sensitivities to surrounding refractive index (SRI) and decreases the sensitivity to temperature after etching of the cladding by HF.[8] Besides, the multimode-interference (MMI) concept has been exploited to the single-mode–multimode–single-mode structure (SMS), and these related characteristics have been studied extensively.[9,10] The SMS band-pass filter parameters, such as center wavelength, bandwidth, and isolation, are discussed with the relationship to the segment length and core size of multimode fiber (MMF).[11] By splicing different MMFs sections in between two single-mode fiber (SMFs), a strain-independent temperature sensor or a temperature-independent strain sensor is demonstrated.[12]

In this study, we proposed a dual-parameter fiber sensor based on cascading a FBG with a hetero-core–structured fiber, which is composed of a short piece of no-core (coreless) fiber (NCF) sandwiched between two SMFs. This configuration will make simple and flexible sensors with a nice response to sense both the temperature and index without the etching and polishing fabrication process. The experimental results well demonstrate that this sensor can monitor two different parameters including temperature and index simultaneously.

## 2 Basic Sensing Principle

The sensing mechanism features a FBG spliced to a hetero-core structure fiber. The FBG is fabricated hydrogen-loaded SMF by using the phase mask writing technique. The hetero-core structure fiber consisting of a NCF spliced between two SMFs is shown in the inset of Fig. 1.

The NCF is a highly pure silica fiber without core manufactured by the Prime Optical Fiber Corporation, Taiwan. When the incident light wave propagates along the axial direction of NCF, the outer medium of the adjacent substance to be sensed with a lower index than the cladding layer index of the fiber facilitates a total internal reflection due to Fresnel reflection. Thus, together with the outer medium, the section of NCF can be equivalently viewed as a MMF with an inner core of 125 $\mu$m in diameter. In this hetero-core structure device, the single-mode light beam traveling in the SMF excites a few guided modes in the NCF, which can support those modes. The excited guided modes can propagate through the NCF and be further coupled to the next spliced SMF. This system is called the well-known MMI filter.[13] According to the MMI theory previously studied, the loss-dip free-space wavelength $\lambda_m$ of interference pattern can be calculated by using:[13]

$$\lambda_m = m\left(\frac{4n_{\mathrm{NCF}}^{\mathrm{eff}}a_{\mathrm{NCF}}^2}{L}\right), \qquad m = 0, 1, 2, 3\ldots, \tag{1}$$

where $L$ is the length of NCF, $m$ represents the self-image number, and $n_{\mathrm{NCF}}^{\mathrm{eff}}$ and $a_{\mathrm{NCF}}$ stand for the effective index and the radius of the NCF, respectively, at the wavelength of $\lambda_m$. Referred to Eq. (1), when the effective index of modes in the NCF is changed by the SRI, the loss-dip wavelength $\lambda_m$ changes proportionally due to that the MMI is strongly influenced by these changes of SRI. For the FBG sensing, due to the waveguide mode being confined to the core, the FBG wavelength $\lambda_B$ is insensitive to the SRI variation. The temperature sensitivity of the FBG is dependent on the coefficient of thermal expansion ($\alpha$), thermo-optic coefficient ($\zeta$), and the FBG effective index.[14]

By using the different sensing characteristics of both the FBG and MMI, the temperature variation $\Delta T$ and the index variation $\Delta n$ can be simultaneously obtained from the measurement wavelength shifts ($\Delta\lambda$) of the Bragg wavelength and

*Address all correspondence to: Guei-Ru Lin, E-mail: p9840375@fcu.edu.tw

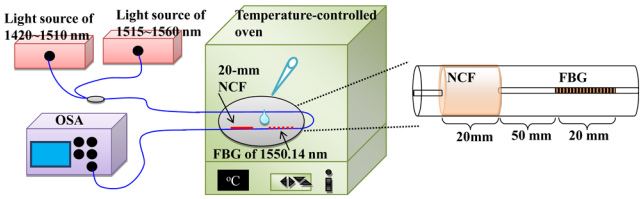


**Fig. 1** The experimental setup with an inset schematic diagram of the proposed no-core fiber fiber Bragg grating (NCF-FBG) sensor for measuring different refractive indices and different temperatures.

the MMI wavelength in the experiments by applying various temperatures and indices to the sensor head.

## 3 Experimental Results and Discussion

The experimental setup is shown in Fig. 1, which comprises the proposed NCF-FBG sensor, two broadband light sources coupled to the fiber via two input ports of a 3-dB fiber Y-coupler whose output end is spliced to the sensing head and an optical spectrum analyzer with the resolution of 0.05 nm (the Advantest Corporation product-type of Q8384, Japan), utilized for monitoring the transmission spectrum from the sensing head. For temperature measurements, the sensing head is placed in a temperature-controlled oven and the chamber temperature could be set by a thermostat. For index measurements, the sensing head is placed on a wafer with droplets of different-index oils on the sensing area with the temperature controlled at 25°C.

The original transmission spectrum of the proposed fiber sensor has two loss-dips taking place at the MMI-wavelength of 1468.36 nm and Bragg-wavelength of 1550.14 nm, respectively. The temperature effect of the proposed sensor has been repeated in the temperature range from 25°C to 120°C. The sensitivities of both the MMI and the FBG are, respectively, 10.97 and 12.73 pm/°C with a nice linear relationship between the temperature and the MMI and FBG wavelength shifts as shown in Fig. 2(a). This result confirms that the wavelength shifts of both the MMI and FBG are linearly proportional to the temperature increment.

The experimental results for different SRIs reveal that the loss-dip wavelength red-shifts as the index increases. This phenomenon is attributed to the interference between the copropagation core and the cladding modes in the NCF. Figure 2(b) indicates the relationship between the loss-dip wavelength shift and the index. For the index ranging from 1.300 to 1.440, the loss-dip wavelength of the MMI is shifted from 1475.9 to 1486.485 nm, which appears to be a sensitivity of 82.598 nm/RIU. At the same time, the Bragg

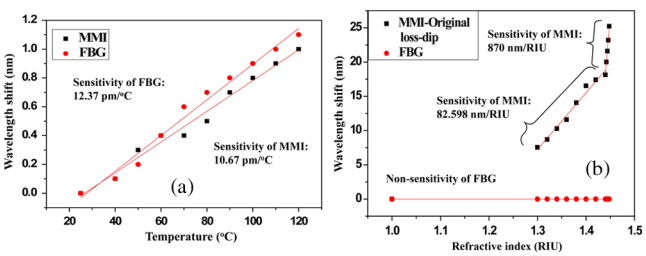


**Fig. 2** The relationship between the loss-dip-wavelength shifts of both the multimode signals' interference (MMI) and the FBG (a) the temperature, (b) the refractive index.

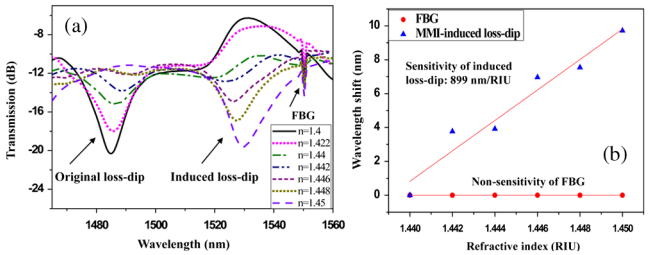


**Fig. 3** (a) The transmission spectra both of MMI and FBG, and (b) the relationship of the loss-dip wavelength shift of the FBG and the MMI-induced loss-dip with different refractive indices in the range from 1.44 to 1.45.

wavelength keeps locating at 1550.285 nm due to the fundamental mode of FBG propagating in the core without being affected by ambient index change.

When the index is increased from 1.400 to 1.450, the transmission spectrum of the MMI is varied as exhibited in Fig. 3(a). As the index of the oil is increased to 1.440, a high-order mode-induced dip starts to be created at a wavelength of 1519.69 nm. The magnitude of the original loss-dip ($\lambda_1 = 1484.89$ nm) becomes shallower and a new induced dip forms as the SRI increases. This phenomenon is due to the fact that index is a function of wavelength, $n(\lambda)$. When the $n_{\text{oil}}$ $(\lambda_1)$ becomes nearly equal to the index of silica $n_{\text{silica}}$ $(\lambda_1)$, the dip-depth of the original loss-dip diminishes. When the index $n_{\text{oil}}$ $(\lambda_1)$ is equal to the index of silica, a loss-dip is induced at 1519.69 nm. This is because the dispersion effect causes the $\lambda_1$ to be shifted to longer wavelengths as the phase-matching condition of the MMI is satisfied.

For the original loss-dip, when the index is increased from 1.440 to 1.448, the corresponding sensitivity is 870 nm/RIU, which is 10 times that of the index range from 1.300 to 1.440 as shown in Fig. 2(b). This tremendous increase in sensitivity is because the SRI is approximately equal to the cladding index of the NCF and the mode indices of the MMI become very sensitive to the SRI. For the induced loss-dip, the corresponding higher (than the original loss-dip's) sensitivity of 899 nm/RIU is obtained in the index range from 1.440 to 1.450 as indicated in Fig. 3(b).

According to the above experimental results, we can see that the device has a good linearity for the wavelength shift affected by the temperature and the SRI. The two unknown physical parameters ($\Delta n$ and $\Delta T$) can be obtained from the given wavelength shift of both FBG and MMI as shown.

$$\begin{bmatrix} \Delta\lambda_{\text{MMI}} \\ \Delta\lambda_{\text{FBG}} \end{bmatrix} = \begin{bmatrix} M_{11} & 0.01067 \\ 0 & 0.01237 \end{bmatrix} \begin{bmatrix} \Delta n \\ \Delta T \end{bmatrix}. \tag{2}$$

For the parameter of $M_{11}$, there are three different values related to three cases. Case I for the original loss-dip: $M_{11} = 82.598$ nm/RIU is obtained in the RI range from 1.300 to 1.440. Also, case II: $M_{11} = 870$ nm/RIU is obtained in the RI range from 1.440 to 1.448. Case III for the induced loss-dip: $M_{11} = 899$ nm/RIU is obtained for the RI range from 1.440 to 1.450. The sensitivity determination depends on the loss-dip wavelength to be shifted in one region (case I or case II region). For an unknown surrounding index measurement, as the total wavelength shift is less than 18 nm, the sensitivity of case I is chosen. The sensitivity of case II is utilized as the total wavelength shift is more than 18 nm.

When an induced loss-dip is created and is employed for the measurement, the sensitivity of case III is resolved. These results clearly reveal that the proposed dual-parameter fiber sensor can be used for versatile and multipurpose sensing applications.

## 4 Conclusions

This sensor including a FBG used in series with a NCF sandwiched between two SMFs demonstrates an innovative and simple sensing scheme. The measured wavelength shifts of the transmission function of the MMI and FBG can be used to detect the variations in the SRI as well as temperature. A transfer matrix provides the determination of the important parameters of the sensor for the device design. Different thin films of sensing materials to be coated on the surface of the NCF will allow more applications in the measurements of indices in the range of different surroundings, such as fluids, chemicals industry, and even bio-chemical fields.

### *Acknowledgments*

The authors would like to specifically thank the National Science Council of the Republic of China, Taiwan, for sponsoring this research under Contract Nos. NSC 102-2917-I-035-005 and NSC 101-2221-E-035-046-MY2.

### *References*

1. H. J. Patrick, A. D. Kersey, and F. Bucholtz, "Analysis of the response of long period fiber gratings to external index of refraction," *J. Lightwave Technol.* **16**(9), 1606–1612 (1998).
2. S. M. Melle, K. Liu, and R. M. Measures, "Strain sensing using a fibre optic Bragg grating," *Proc. SPIE* **1588**, 255–263 (1991).
3. K. Wen et al., "Design of fiber Bragg gratings with arbitrary reflective spectrum," *Opt. Eng.* **50**(5), 054003 (2011).
4. X. Zou et al., "All-fiber optical filter with an ultranarrow and rectangular spectral response," *Opt. Lett.* **38**(16), 3096–3098 (2013).
5. X. Shu et al., "Sampled fiber Bragg grating for simultaneous refractive-index and temperature measurement," *Opt. Lett.* **26**(11), 774–776 (2001).
6. B. O. Guan et al., "Simultaneous strain and temperature measurement using a superstructure fiber Bragg grating," *IEEE Photonics Technol. Lett.* **12**(6), 675–677 (2000).
7. H. J. Patrick et al., "Hybrid fiber Bragg grating/long period fiber grating sensor for strain/temperature discrimination," *IEEE Photonics Technol. Lett.* **8**(9), 1223–1225 (1996).
8. X. Chen et al., "Simultaneous measurement of temperature and external refractive index by use of a hybrid grating in D fiber with enhanced sensitivity by HF etching," *Appl. Opt.* **44**(2), 178–182 (2005).
9. Q. Wang, G. Farrell, and W. Yan, "Investigation on single-mode–multimode–single-mode fiber structure," *J. Lightwave Technol.* **26**(5), 512–519 (2008).
10. W. S. Mohammed, A. Mehta, and E. G. Johnson, "Wavelength tunable fiber lens based on multimode interference," *J. Lightwave Technol.* **22**(2), 469–477 (2004).
11. W. S. Mohammed and P. W. E. Smith, "All-fiber multimode interference bandpass filter," *Opt. Lett.* **31**(17), 2547–2549 (2006).
12. S. M. Tripathi et al., "Strain and temperature sensing characteristics of single-mode–multimode–single-mode structures," *J. Lightwave Technol.* **27**(13), 2348–2356 (2009).
13. J. E. Antonio-Lopez et al., "Tunable multimode-interference bandpass fiber filter," *Opt. Lett.* **35**(3), 324–326 (2010).
14. R. Kashyap, *Fiber Bragg Grating*, Academic Press, Canada (2010).